Terahertz radiation, circular dichroism, and optical activity of a Rashba quantum ring subjected to a static electric field

Omid Sharifi Sedeh and MirFaez Miri*
Department of Physics, University of Tehran, P.O. Box 14395-547, Tehran, Iran

(Received 7 October 2019; revised manuscript received 29 November 2019; published 19 December 2019)

We study a Rashba quantum ring subjected to an in-plane static electric field. Due to the violation of the rotational symmetry, the system radiates at the Rabi frequency upon interaction with a strong electromagnetic field. With a proper choice of the driving amplitude, the radiation frequency is in the range of $0.1 - 10$ THz. Due to the Rashba spin-orbit interaction which splits the spin-up and spin-down states and affects the transitions between the ground and excited states, the system exhibits circular dichroism and optical activity. The static electric field and gate-voltage-dependent Rashba parameter strongly influence the system. In other words, the Rashba quantum ring may serve as an *electrically tunable* terahertz emitter, absorption modulator, dichroic element, and polarization rotator.

DOI: 10.1103/PhysRevB.100.235434

I. INTRODUCTION

The terahertz (THz) region of the electromagnetic spectrum ($\sim$0.1 to 10 THz) has attracted increasing attention during the past two decades [1,2]. One of the reasons of interest in the so-called THz gap is the potential of THz spectroscopy to study the structure and dynamics of condensed matter systems. Indeed photons of energy $\sim$0.4 to 40 meV are able to probe the *low-energy* excitations of condensed matter systems. Several spectroscopic studies are devoted to the opening of a superconducting gap in MgB_2 [3], energy levels of excitons in GaAs quantum wells [4], and spin waves in antiferromagnetic NiO [5], to name only a few.

Recent years have witnessed remarkable progress in the development of THz sources, detectors, and optical components [1,2]. However, existing THz systems have their own limitations; for example, free-electron-based sources are bulky and expensive, Gunn diode or tunnel injection transit-time diode-based oscillators cover only the lower boundary of the THz region [6], and quantum cascade lasers operate only at cryogenic temperatures. To address the optimization of cost, size, mass producibility, as well as operation temperature, spectral characteristics, and output power, solid-state THz sources are introduced [7–11], such as those based on hot electrons in single-walled carbon nanotubes [7], resonant interlayer radiative transitions in double-graphene-layer structure [8], and transitions of exciton polaritons confined in a parabolic potential trap in a semiconductor microcavity [9].

Semiconductor nanostructures such as quantum dots and quantum wells are promising for the realization of THz sources and detectors: Indeed, the quantized electronic states of these so-called artificial atoms can be engineered [12]. While quantum states with an energy difference within the THz range are achievable, electric dipole transition between states of the same parity is forbidden. This can be remedied by breaking the inversion symmetry of the potential that confines the electrons and holes [13]. Exposed to a strong coherent pump, energy levels of the artificial atom hybridize with the electromagnetic field and split into AC-Stark split doublets. In asymmetric artificial atoms, the electric dipole transition between two states of the same doublet leads to emission at the Rabi frequency. Since the Rabi frequency is proportional to the pump amplitude, THz emission is achievable. Along this line of thought, III-nitride quantum dots with built-in strain-induced electric field breaking the inversion symmetry are studied [13]. The dipole moment of such an asymmetric quantum dot is $\sim$10 Debye, thus for pump amplitudes $\sim 10^7$ V/m the THz radiation is observable. A scheme of THz laser based on an ensemble of asymmetric quantum dots in a high-Q photonic crystal cavity is proposed [14]. Intersubband transitions in an asymmetric quantum well are also explored [15]. Here the effective dipole moment $\sim$60 Debye permits THz radiation at lower pump amplitudes $\sim 10^6$ V/m. It is further shown that an array of *tunneling coupled* asymmetric artificial atoms allows THz emission in a broad range [16,17]. For example, the radiation frequency of seven coupled asymmetric artificial atoms increases from 3.0 to 6.36 THz as the tunneling energy increases from zero to 2 meV. In the following, we focus on *quantum rings* rather than quantum dots and quantum wells, in view of THz emitters operating at low driving fields $\sim 10^5$ V/m.

Progress in self-organized growth, droplet epitaxy, and lithographic patterning have made it possible to fabricate quantum rings [18,19]. From a topological point of view, a ring is a doubly connected structure. Thus, a quantum ring offers a unique possibility to explore topological quantum effects. The most prominent example is the Aharonov-Bohm effect [20], in which the magnetic flux breaks the equivalence of clockwise and counterclockwise electron paths around a ring symmetrically connected to two external leads. This gives rise to flux-dependent interference of electron wave packets

*mirfaez_miri@ut.ac.ir

that can take two distinct paths around the ring. Not only the Aharonov-Bohm effect but also the Aharonov-Casher effect [21] in ringlike structures are experimentally demonstrated [22–26]. The electric analog of the Aharonov-Bohm effect, the Aharonov-Casher effect, is due to the effective magnetic field induced by the *spin-orbit interaction*. After the introduction of modulation-doped semiconductor heterostructures, the prominence of the odd in electron's momentum Rashba spin-orbit coupling has been shown in a variety of structures that lack inversion symmetry [27–29]. Quite remarkably, the Rashba spin-orbit interaction strength can be controlled by an external gate voltage [30–34]. This renders the Rashba spin-orbit interaction quite attractive since the electric field control of spin states is preferable to magnetic field control.

Recently, there has been growing interest in the interaction of quantum rings with electromagnetic waves [35–42]. To achieve electric dipole transition between quantum states with an energy difference within the THz range, Alexeev and Portnoi considered a quantum ring pierced by a magnetic flux and under a lateral electric field [36]. For a ring of radius 20 nm, magnetic field ∼3 T, and static electric field $\sim 10^4$ V/m, the transition frequency is ∼0.5 THz. However, the use of a magnetic field introduces difficulties in the design of an inexpensive, compact, and portable quantum-ring-based THz source.

In this paper, we consider a quantum ring with the *Rashba spin-orbit interaction* subjected to an in-plane static electric field. The external electric field breaks the rotational symmetry of the system, and thus each energy eigenstate can be regarded as a superposition of angular momentum eigenstates [36]. Violation of the rotational symmetry has an immediate consequence: The system behaves as a giant asymmetric artificial atom. Interacting with a strong electromagnetic field, the Rashba quantum ring radiates at the Rabi frequency. Thus, with an appropriate choice of the driving amplitude, THz emission is achievable. Indeed, the external static electric field and the gate-voltage-dependent Rashba parameter can be used to tune the Rabi frequency. For example, for an InGaAs quantum ring of radius 85 nm, Rashba parameter 0.08 eVÅ, driving field 10^5 V/m, and static electric field <35 V/m, the radiation frequency is in the range of 0.1−9.1 THz which is almost the whole THz gap. To develop THz emitters based on dressed artificial atoms, quantum dots and quantum wells may be inferior to Rashba quantum rings which offer low driving field, broad radiation frequency range, and electrical tunability. On the other hand, the Rashba spin-orbit interaction locks the spin and momentum degrees of freedom, splits the spin-up and spin-down states, and influences optical transitions between the ground and excited states. Due to the Rashba spin-orbit interaction, the system exhibits circular dichroism and optical activity which markedly depend on the gate voltage and external electric field. In other words, the Rashba quantum ring may serve as an *electrically tunable* absorption modulator, dichroic element, and polarization rotator operating in the THz region of the electromagnetic spectrum.

II. MODEL

We consider an electron confined in a quantum ring of radius r_c, under the action of a static electric field $\mathbf{E}_s = E_s\hat{\mathbf{e}}_x$,

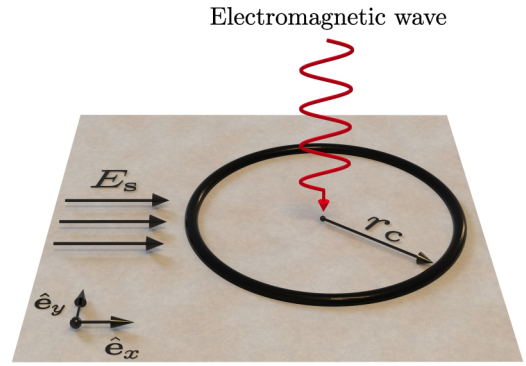

FIG. 1. The schematics of a quantum ring subjected to a static electric field and an electromagnetic wave.

and a plane wave with electric field and magnetic induction,

$$\mathbf{E}(\mathbf{r},t) = \mathrm{Re}(E_p\hat{\mathbf{e}}_p e^{i\mathbf{k}_p\cdot\mathbf{r}-i\omega_p t}),$$
$$\mathbf{B}(\mathbf{r},t) = \mathrm{Re}\left(\frac{E_p}{\omega_p}\mathbf{k}_p\times\hat{\mathbf{e}}_p e^{i\mathbf{k}_p\cdot\mathbf{r}-i\omega_p t}\right), \quad (1)$$

respectively. Here ω_p is the frequency, $\hat{\mathbf{e}}_p$ is the polarization vector, and $\mathbf{k}_p$ is the wave vector of the incident wave. We assume that $\mathbf{k}_p = k_p\hat{\mathbf{e}}_z$, that is, the wave vector is perpendicular to the ring (see Fig. 1). We pay special attention to linearly polarized waves with polarization vectors $\hat{\mathbf{e}}_x$ and $\hat{\mathbf{e}}_y$, and circularly polarized waves with polarization vectors $\hat{\mathbf{e}}_+ = -\frac{1}{\sqrt{2}}(\hat{\mathbf{e}}_x + i\hat{\mathbf{e}}_y)$ and $\hat{\mathbf{e}}_- = +\frac{1}{\sqrt{2}}(\hat{\mathbf{e}}_x - i\hat{\mathbf{e}}_y)$.

The two-dimensional Hamiltonian for an electron in the presence of Rashba spin-orbit interaction and external fields is

$$\mathcal{H}^{2D} = \frac{(\mathbf{p}+e\mathbf{A})^2}{2m^*} - e\Phi(\mathbf{r}) + \frac{\alpha_R}{\hbar}\hat{\mathbf{e}}_z\cdot[\boldsymbol{\sigma}\times(\mathbf{p}+e\mathbf{A})] + V(\mathbf{r}) + e\mathbf{r}\cdot\mathbf{E}_s, \quad (2)$$

where $-e<0$ is the electron charge, m_e is the electron mass, m^* is the electron effective mass, α_R is the Rashba parameter, σ_x and σ_y are Pauli matrices, $\mathbf{r}=(x,y)=(r\cos\theta, r\sin\theta)$ is the position vector, and $\mathbf{p}=(p_x,p_y)$ is the momentum vector. The scalar potential $\Phi(\mathbf{r},t)$ and the vector potential $\mathbf{A}(\mathbf{r},t)$ determine $\mathbf{E} = -\nabla\Phi - \partial\mathbf{A}/\partial t$ and $\mathbf{B} = \nabla\times\mathbf{A}$. The strong potential $V(\mathbf{r})$ forces the electron wave function to be localized on the ring. This allows us to derive an effective *one-dimensional* Hamiltonian to describe the system.

III. DERIVATION OF THE ONE-DIMENSIONAL HAMILTONIAN

It is well known that the fields $\mathbf{E}$ and $\mathbf{B}$ are invariant under the transformations $\Phi\to\Phi-\partial\chi/\partial t$ and $\mathbf{A}\to\mathbf{A}+\nabla\chi$, where χ is an arbitrary function. To remove the ambiguity caused by the freedom of gauge, we express the Hamiltonian $\mathcal{H}^{2D}$ in terms of fields $\mathbf{E}$ and $\mathbf{B}$. We follow Barron and Gray [43,44] to write

$$\Phi(\mathbf{r},t) = \Phi_0(t) - r_\alpha E_{0\alpha}(t) - \tfrac{1}{2}r_\alpha r_\beta\partial_\beta E_{0\alpha}(t) + \ldots,$$
$$A_\alpha(\mathbf{r},t) = \tfrac{1}{2}\epsilon_{\alpha\beta\gamma}r_\gamma B_{0\beta}(t) + \tfrac{1}{3}\epsilon_{\alpha\gamma\lambda}r_\beta r_\lambda\partial_\beta B_{0\gamma}(t) + \ldots,$$

where $E_{0\alpha}$, $\partial_\beta E_{0\alpha}$, etc., are all evaluated at the origin $\mathbf{r}=\mathbf{0}$. We assume that $k_{\rm p}r_{\rm c}\ll 1$. It follows that the Hamiltonian can be written as

$$\mathcal{H}^{\rm 2D}=\frac{\mathbf{p}^2}{2m^*}+V(\mathbf{r})+\frac{\alpha_{\rm R}}{\hbar}\hat{\mathbf{e}}_z\cdot(\boldsymbol{\sigma}\times\mathbf{p})+e\mathbf{r}\cdot\mathbf{E}_{\rm s}+e\mathbf{r}\cdot\mathbf{E}(\mathbf{0},t), \tag{3}$$

within the dipole approximation. Note that due to the geometry of the system, terms such as $\frac{e}{2m^*}(\mathbf{r}\times\mathbf{p})\cdot\mathbf{B}(\mathbf{0},t)$ are absent in the above Hamiltonian.

In a naive approach to the effective one-dimensional Hamiltonian of an electron moving on a ring, one sets the cylindrical coordinate r equal to $r_{\rm c}$ and discards all terms proportional to derivatives with respect to r. This approach leads to a non-Hermitian Hamiltonian. Thus, we follow Meijer *et al.* [45] to obtain the correct effective Hamiltonian. Without loss of generality, we assume that the confining potential is $V(\mathbf{r})=\frac{1}{2}k_{\rm c}(r-r_{\rm c})^2$. We write $\mathcal{H}^{\rm 2D}=\mathcal{H}_0^{\rm 2D}+\mathcal{H}_1^{\rm 2D}$, where $\mathcal{H}_0^{\rm 2D}=-\frac{\hbar^2}{2m^*}(\frac{\partial^2}{\partial r^2}+\frac{1}{r}\frac{\partial}{\partial r})+V(\mathbf{r})$. To a good approximation, the lowest energy eigenfunction of $\mathcal{H}_0^{\rm 2D}$ is

$$R_{\rm MMK}(r)=\left(\frac{\gamma_{\rm c}}{\sqrt{\pi}r_{\rm c}}\right)^{\frac{1}{2}}e^{-\frac{1}{2}\gamma_{\rm c}^2(r-r_{\rm c})^2}, \tag{4}$$

when $\gamma_{\rm c}=(m^*k_{\rm c}/\hbar^2)^{\frac{1}{4}}\to\infty$. In the case of a narrow quantum ring, the electron is in the lowest energy radial state. It follows that the effective one-dimensional Hamiltonian is $\mathcal{H}(\theta)=\langle R_{\rm MMK}|\mathcal{H}_1^{\rm 2D}|R_{\rm MMK}\rangle$. Of great use is the identity $\langle R_{\rm MMK}|\frac{\partial}{\partial r}|R_{\rm MMK}\rangle=-\frac{1}{2r_{\rm c}}$. Indeed, this result is independent of the precise shape of the strong confining potential and the lowest energy radial mode [45]. Now it is straightforward to show that $\mathcal{H}=\mathcal{H}_{\rm MMK}+\mathcal{H}_{\rm s}+\mathcal{H}_{\rm p}$, where

$$\begin{aligned}\mathcal{H}_{\rm MMK}=&-\frac{\hbar^2}{2m^*r_{\rm c}^2}\frac{\partial^2}{\partial\theta^2}-\frac{i\alpha_{\rm R}}{r_{\rm c}}\Big((\cos\theta\sigma_x+\sin\theta\sigma_y)\frac{\partial}{\partial\theta}\\&-\frac{1}{2}(\sin\theta\sigma_x-\cos\theta\sigma_y)\Big),\\ \mathcal{H}_{\rm s}=&\,eE_{\rm s}r_{\rm c}\cos\theta,\\ \mathcal{H}_{\rm p}=&-\boldsymbol{\mu}\cdot\left(\frac{E_{\rm p}}{2}\hat{\mathbf{e}}_{\rm p}^*e^{+i\omega_{\rm p}t}+\frac{E_{\rm p}}{2}\hat{\mathbf{e}}_{\rm p}e^{-i\omega_{\rm p}t}\right).\end{aligned} \tag{5}$$

$\mathcal{H}_{\rm MMK}$ is the one-dimensional Hamiltonian for an electron on a quantum ring, which includes the Rashba spin-orbit interaction [45]. $\mathcal{H}_{\rm s}$ expresses the influence of the external static electric field. $\boldsymbol{\mu}=-er_{\rm c}(\cos\theta\hat{\mathbf{e}}_x+\sin\theta\hat{\mathbf{e}}_y)$ is the electric dipole moment. $\mathcal{H}_{\rm p}$ expresses the interaction of an electron with the electromagnetic field.

IV. CIRCULAR DICHROISM OF A RASHBA QUANTUM RING

First we consider a quantum ring in the absence of the Rashba interaction and external fields. The eigenfunction and eigenenergy of the Hamiltonian $\mathcal{H}=-\frac{\hbar^2}{2m^*r_{\rm c}^2}\frac{\partial^2}{\partial\theta^2}$ are $\psi_\ell(\theta)=\frac{1}{\sqrt{2\pi}}e^{i\ell\theta}$ and $\mathcal{E}_\ell=\frac{\hbar^2\ell^2}{2m^*r_{\rm c}^2}$, where $\ell=0,\pm1,\pm2,\ldots$. The sign of the group velocity $\hbar\ell/(m^*r_{\rm c})$ determines the direction of electron propagation around the ring.

Next, we revisit a Rashba quantum ring under no external fields [19]. The eigenspinor $\psi_{\ell,s}(\theta)$ and eigenenergy $\mathcal{E}_{\ell,s}^{\rm MMK}=\hbar^2\epsilon_{\ell,s}^{\rm MMK}/(2m^*r_{\rm c}^2)$ of the Hamiltonian $\mathcal{H}_{\rm MMK}$ are

$$\begin{aligned}\psi_{\ell,s}(\theta)&=\frac{1}{\sqrt{2\pi}}e^{i\ell\theta}\begin{pmatrix}\chi_{\ell,s}\\ \zeta_{\ell,s}e^{i\theta}\end{pmatrix},\\ \epsilon_{\ell,s}^{\rm MMK}&=\left(\ell+\frac{1}{2}\right)^2+\frac{1}{4}+s\sqrt{\left(\ell+\frac{1}{2}\right)^2\left(1+Q_R^2\right)},\end{aligned} \tag{6}$$

where $\ell=0,\pm1,\pm2,\ldots$, $s=\pm1$, $Q_R=2m^*\alpha_{\rm R}r_{\rm c}/\hbar^2$, $\mathrm{sgn}(\ell)=\ell/|\ell|$, and

$$\begin{aligned}\chi_{\ell,+1}=&-\zeta_{\ell,-1}=\frac{Q_R\mathrm{sgn}\left(\ell+\frac{1}{2}\right)}{\sqrt{Q_R^2+\left[1+\mathrm{sgn}\left(\ell+\frac{1}{2}\right)\sqrt{1+Q_R^2}\right]^2}},\\ \zeta_{\ell,+1}=&+\chi_{\ell,-1}=\frac{\left[1+\mathrm{sgn}\left(\ell+\frac{1}{2}\right)\sqrt{1+Q_R^2}\right]\mathrm{sgn}\left(\ell+\frac{1}{2}\right)}{\sqrt{Q_R^2+\left[1+\mathrm{sgn}\left(\ell+\frac{1}{2}\right)\sqrt{1+Q_R^2}\right]^2}}.\end{aligned} \tag{7}$$

Noticeably $\epsilon_{\ell,s}^{\rm MMK}=\epsilon_{-\ell-1,s}^{\rm MMK}$, in other words, the states $\psi_{\ell,s}$ and $\psi_{-\ell-1,s}$ are degenerate.

The external static electric field breaks the rotational symmetry of the system, nevertheless, the eigenspinors are 2π periodic in θ. To solve the Schrödinger equation $(\mathcal{H}_{\rm MMK}+\mathcal{H}_{\rm s})\Psi(\theta)=\mathcal{E}\Psi(\theta)$, we write the eigenspinor $\Psi(\theta)$ as a linear combination of the spinors $\psi_{\ell,s}(\theta)$, that is,

$$\Psi(\theta)=\sum_{\ell,s}c_{\ell,s}\psi_{\ell,s}(\theta). \tag{8}$$

The Schrödinger equation can be written as

$$\sum_{\ell,s}c_{\ell,s}\left(\epsilon_{\ell,s}^{\rm MMK}-\epsilon+2E_{\rm ss}\cos\theta\right)e^{i\ell\theta}\begin{pmatrix}\chi_{\ell,s}\\ \zeta_{\ell,s}e^{i\theta}\end{pmatrix}=0, \tag{9}$$

where $\epsilon=2m^*r_{\rm c}^2\mathcal{E}/\hbar^2$ and $E_{\rm ss}=eE_{\rm s}r_{\rm c}^3m^*/\hbar^2$ are the scaled energy and scaled static electric field, respectively. Multiplying this equation by $\psi_{\ell',s'}^*(\theta)$ and intergating over θ, leads to the following eigenproblem:

$$\sum_{\ell,s}c_{\ell,s}\left[\left(\epsilon_{\ell,s}^{\rm MMK}-\epsilon\right)\delta_{\ell,\ell'}+E_{\rm ss}(\delta_{\ell,\ell'+1}+\delta_{\ell,\ell'-1})\right]\Lambda_{\ell,s}^{\ell',s'}=0, \tag{10}$$

where $\Lambda_{\ell,s}^{\ell',s'}=\chi_{\ell',s'}^*\chi_{\ell,s}+\zeta_{\ell',s'}^*\zeta_{\ell,s}$. In practice, we consider $\ell=0,\pm1,\pm2,\ldots,\pm\ell_{\rm max}$ in the expansion Eq. (8). Even for large static electric fields, the eigenspinors and eigenenergies of the Hamiltonian $\mathcal{H}_{\rm MMK}+\mathcal{H}_{\rm s}$ can be obtained if one chooses an adequate set of basis spinors. To simplify the computations, it is worth noting that $\Lambda_{-1,+1}^{0,+1}=\Lambda_{-1,-1}^{0,-1}=0$, $\Lambda_{-1,-1}^{0,+1}=-\Lambda_{-1,+1}^{0,-1}=1$, $\Lambda_{0,s}^{0,s'}=\delta_{s,s'}$, and $\Lambda_{\ell,s}^{\ell',s'}=\delta_{s,s'}$ if $\mathrm{sgn}(\ell')\mathrm{sgn}(\ell)>0$ and $\ell\ell'\neq0$.

As mentioned before, the interaction of the electromagnetic field and the quantum ring can be described by the Hamiltonian $\mathcal{H}_{\rm p}=\mathcal{V}e^{i\omega_{\rm p}t}+\mathcal{V}^\dagger e^{-i\omega_{\rm p}t}$, where $\mathcal{V}=-\frac{1}{2}E_{\rm p}\boldsymbol{\mu}\cdot\hat{\mathbf{e}}_{\rm p}^*$. According to Fermi's golden rule, the transition rate between the initial electron state $|\Psi_i\rangle$ and the final electron state

$|\Psi_f\rangle$ is

$$W_{i\to f} = \frac{2\pi}{\hbar}|\langle\Psi_f|\mathcal{V}^\dagger|\Psi_i\rangle|^2\delta(\mathcal{E}_f - \mathcal{E}_i - \hbar\omega_\mathrm{p}), \tag{11}$$

where $\mathcal{E}_f > \mathcal{E}_i$ is assumed. The total upward transition rate is $R_\mathrm{abs} = \sum_f W_{i\to f}$. The intensity of the incident electromagnetic wave is $\mathscr{P}_\mathrm{av} = n_\mathrm{h} c\epsilon_0 E_\mathrm{p}^2/2$. Here c is the speed of light in free space, ϵ_0 is the permittivity of free space, and n_h is the refractive index of the host semiconductor. The fraction of photons absorbed by the ring is

$$\alpha(\hbar\omega_\mathrm{p}) = \frac{R_\mathrm{abs}}{\mathscr{P}_\mathrm{av}\pi r_\mathrm{c}^2/(\hbar\omega_\mathrm{p})}. \tag{12}$$

It is convenient to introduce the scaled absorption coefficient $\alpha_\mathrm{scaled}(\hbar\omega_\mathrm{p}) = \frac{n_\mathrm{h}\hbar c\varepsilon_0}{e^2}\alpha(\hbar\omega_\mathrm{p})$. To this end,

$$\alpha_\mathrm{scaled}(\hbar\omega_\mathrm{p}) = \sum_f \hbar\omega_\mathrm{p}|\hat{\mathbf{e}}_\mathrm{p}\cdot\langle\Psi_f|(\cos\theta\hat{e}_x + \sin\theta\hat{e}_y)|\Psi_i\rangle|^2 \times L(\mathcal{E}_f - \mathcal{E}_i - \hbar\omega_\mathrm{p}). \tag{13}$$

Note that to take into account the width of the energy levels, we have used the Lorentzian function

$$L(\mathcal{E}_f - \mathcal{E}_i - \hbar\omega_\mathrm{p}) = \frac{\Gamma/\pi}{(\mathcal{E}_f - \mathcal{E}_i - \hbar\omega_\mathrm{p})^2 + \Gamma^2} \tag{14}$$

rather than the delta function $\delta(\mathcal{E}_f - \mathcal{E}_i - \hbar\omega_\mathrm{p})$. To quantify the linear and circular dichroism of the Rashba quantum ring, we use

$$\begin{aligned}\mathrm{LD}_\mathrm{scaled} &= \alpha_\mathrm{scaled}(\hat{\mathbf{e}}_\mathrm{p} = \hat{\mathbf{e}}_y) - \alpha_\mathrm{scaled}(\hat{\mathbf{e}}_\mathrm{p} = \hat{\mathbf{e}}_x),\\ \mathrm{CD}_\mathrm{scaled} &= \alpha_\mathrm{scaled}(\hat{\mathbf{e}}_\mathrm{p} = \hat{\mathbf{e}}_+) - \alpha_\mathrm{scaled}(\hat{\mathbf{e}}_\mathrm{p} = \hat{\mathbf{e}}_-).\end{aligned} \tag{15}$$

In the absence of *both* the Rashba interaction and external static electric field, a quantum ring prepared in the ground state ψ_0 does *not* exhibit either linear or circular dichroism. In this case, the scaled absorption coefficient is the same,

$$\alpha_\mathrm{scaled}(\hbar\omega_\mathrm{p}) = \frac{\hbar\omega_\mathrm{p}}{2}L(\mathcal{E}_{\pm1} - \hbar\omega_\mathrm{p}),$$

for polarization vectors $\hat{\mathbf{e}}_x$, $\hat{\mathbf{e}}_y$, $\hat{\mathbf{e}}_+$, and $\hat{\mathbf{e}}_-$. The linear dichroism emerges as one introduces the symmetry breaking static electric field $\mathbf{E}_\mathrm{s} = E_\mathrm{s}\hat{\mathbf{e}}_x$: Indeed the absorption coefficient depends on the initial state and all possible final states excited by the incident wave [see Eq. (13)]. In the absence (presence) of the static electric field, the eigenstates are (are not) characterized by a particular value of angular momentum quantum number, and this strongly influences the *polarization-dependent* transition amplitude. Even in the absence of the static electric field, the Rashba quantum ring exhibits circular dichroism. The circular dichroism of the system is due to the Rashba spin-orbit interaction which locks the spin and momentum degrees of freedom, splits the spin-up and spin-down states, and dictates the selection rules for the optical transitions: When $\mathbf{E}_\mathrm{s} = 0$, a circularly polarized wave with the polarization vector $\hat{\mathbf{e}}_+$ ($\hat{\mathbf{e}}_-$) gives rise to transition from the ground state $\psi_{0,-1}$ to the excited state $\psi_{1,-1}$ ($\psi_{-1,1}$). On the other hand, $\mathcal{E}^\mathrm{MMK}_{1,-1} \neq \mathcal{E}^\mathrm{MMK}_{-1,1}$ while $\mathcal{E}_1 = \mathcal{E}_{-1}$. In this case, the circular dichroism of the system is

$$\mathrm{CD}_\mathrm{scaled}(\hbar\omega_\mathrm{p}) = \frac{\hbar\omega_\mathrm{p}}{2}\big[L\big(\mathcal{E}^\mathrm{MMK}_{1,-1} - \mathcal{E}^\mathrm{MMK}_{0,-1} - \hbar\omega_\mathrm{p}\big) - L\big(\mathcal{E}^\mathrm{MMK}_{-1,1} - \mathcal{E}^\mathrm{MMK}_{0,-1} - \hbar\omega_\mathrm{p}\big)\big].$$

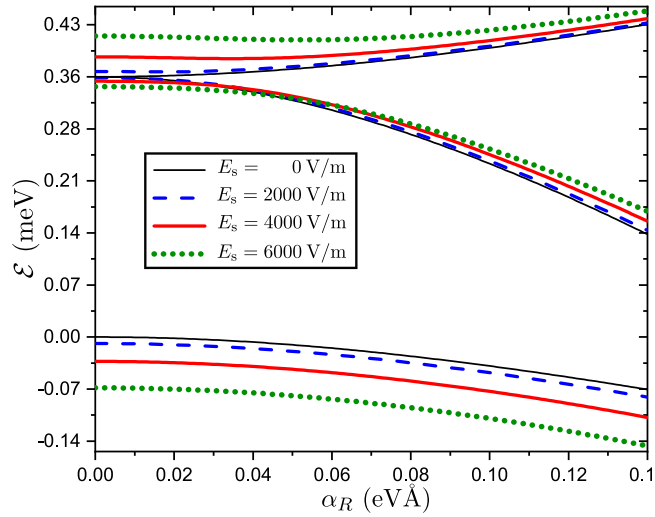

FIG. 2. The three lowest energy levels of a quantum ring versus the Rashba parameter for various static electric fields. Here $m^* = 0.067m_e$ and $r_\mathrm{c} = 40$ nm.

As a concrete example, we consider the experimentally well studied InGaAs quantum ring [46–49]. We take $m^* = 0.067m_e$ for the electron effective mass [47] and $r_\mathrm{c} = 40$ nm for the radius of the ring. Recent advances suggest that such large quantum rings are not out of reach [50]. For the highest electric field strength, we take $E_\mathrm{s} = 8000$ V/m, which leads to a mere potential drop $2r_\mathrm{c}E_\mathrm{s} = 0.64$ mV across the quantum ring. Inspired by the experiments [30,31], we assume that $0 < \alpha_\mathrm{R} < 0.14$ eVÅ. Indeed, the Rashba parameter can be controlled by a gate voltage [31–34]. Figure 2 shows the three lowest doubly degenerate energy levels as a function of the Rashba parameter, for various static electric fields. The ground (second excited) eigenenergy decreases (increases) as the static electric field or the Rashba parameter increases. The first excited eigenenergy does not strongly depend on the static electric field but decreases as the Rashba parameter increases. It follows that the static electric field and the Rashba parameter can be employed to engineer the absorption spectrum of the quantum ring. Quite remarkably, the energy separation between the ground state and two excited states is about 0.4 meV. This indicates that the Rashba quantum ring may exhibit considerable optical response at frequencies about 0.1 THz.

Figures 3(a) and 3(b) demonstrate α_scaled as a function of ω_p, for polarization vectors $\hat{\mathbf{e}}_x$ and $\hat{\mathbf{e}}_y$, respectively. Here $\alpha_\mathrm{R} = 0.08$ eVÅ, $\Gamma = 0.01$ meV, and the initial electron wave function is Ψ_I (see Appendix). The first (second) peak of α_scaled is due to the transition from the ground state to the first (second) excited state. The quantum ring exhibits dichroism: Whether the incident wave is polarized along $\hat{\mathbf{e}}_x$ or $\hat{\mathbf{e}}_y$ has a clear effect on the heights of the peaks of the absorption spectrum. Moreover, the external static electric field has a profound influence on the system. For example, in the case of $\hat{\mathbf{e}}_\mathrm{p} = \hat{\mathbf{e}}_x$, the first and second peaks of α_scaled shift from $\frac{\omega_\mathrm{p}}{2\pi} = 0.076$ and 0.101 THz to 0.104 and 0.139 THz, respectively, and the first peak decreases by a factor about 0.13, as the static electric field increases from 2000 to 8000 V/m. Figures 3(c) and 3(d) show similar plots for polarization vectors $\hat{\mathbf{e}}_+$ and

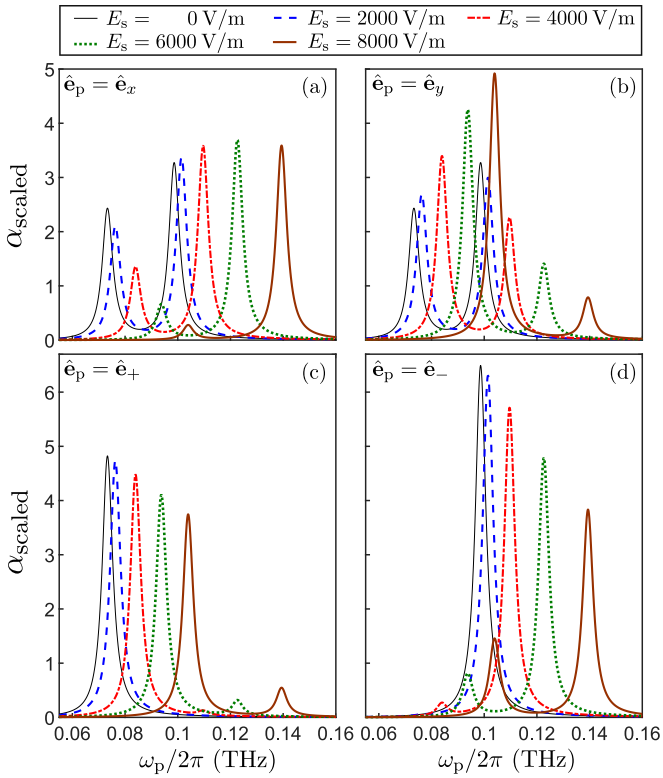

FIG. 3. $\alpha_{\rm scaled}$ as a function of $\omega_{\rm p}$. The polarization vector of the incident wave is (a) $\hat{\mathbf{e}}_x$, (b) $\hat{\mathbf{e}}_y$, (c) $\hat{\mathbf{e}}_+$, and (d) $\hat{\mathbf{e}}_-$. Here $m^*=0.067m_e$, $r_c=40$ nm, $\alpha_R=0.08$ eVÅ, and $\Gamma=0.01$ meV. The initial electron wave function is Ψ_I.

$\hat{\mathbf{e}}_-$, respectively. The quantum ring may absorb light of one circular polarization but not the other. For example, when $E_s=0$ and $\frac{\omega_p}{2\pi}=0.076$ THz, the quantum ring considerably absorbs light of circular polarization $\hat{\mathbf{e}}_+$ but not $\hat{\mathbf{e}}_-$. Here again, the external static electric field has an apparent effect on the absorption and circular dichroism spectra. We conclude that a Rashba quantum ring may serve as a THz electroabsorption modulator or a THz electroabsorption switch which is sensitive to the polarization of the incident wave.

Figure 4 vividly demonstrates that both the Rashba parameter and the external static electric field strongly influence the magnitude and position of the first two peaks of $\rm LD_{scaled}$ and $\rm CD_{scaled}$. We deduce that a Rashba quantum ring may serve as an electrically tunable THz dichroic element.

V. ELECTRICALLY TUNABLE TERAHERTZ RADIATION OF A RASHBA QUANTUM RING

Now we consider the case that only two states $|\Psi_i\rangle$ and $|\Psi_f\rangle$ are mainly involved in the interaction with the electromagnetic wave. We model the quantum ring as a two-level system (TLS) with the Hamiltonian

$$\mathcal{H}_{\rm TLS}=\frac{\hbar\omega_{fi}}{2}(|\Psi_f\rangle\langle\Psi_f|-|\Psi_i\rangle\langle\Psi_i|)+\mathcal{V}e^{i\omega_p t}+\mathcal{V}^\dagger e^{-i\omega_p t}, \quad (16)$$

where $\hbar\omega_{fi}=\mathcal{E}_f-\mathcal{E}_i$ and $\mathcal{V}=\mathcal{V}_{ii}|\Psi_i\rangle\langle\Psi_i|+\mathcal{V}_{if}|\Psi_i\rangle\langle\Psi_f|+\mathcal{V}_{fi}|\Psi_f\rangle\langle\Psi_i|+\mathcal{V}_{ff}|\Psi_f\rangle\langle\Psi_f|$. Quite remarkably, in the presence of the static electric field, the states $|\Psi_i\rangle$ and $|\Psi_f\rangle$ are not characterized by a particular value of quantum number ℓ

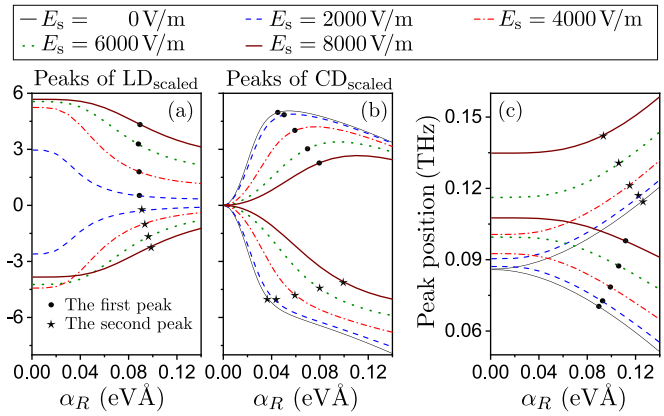

FIG. 4. Peak magnitudes of (a) $\rm LD_{scaled}$ and (b) $\rm CD_{scaled}$, and (c) peak positions of $\rm LD_{scaled}$ and $\rm CD_{scaled}$, as a function of the Rashba parameter for various static electric fields. The parameters are the same as in Fig. 3.

[see Eqs. (6) and (8)]; hence, in general, $\mathcal{V}_{ii}\neq 0$ and $\mathcal{V}_{ff}\neq 0$. It will turn out that the asymmetry parameter

$$\kappa e^{i\xi}=\frac{2(\mathcal{V}_{ii}-\mathcal{V}_{ff})}{\hbar\omega_p}=\frac{E_p(\boldsymbol{\mu}^{ff}-\boldsymbol{\mu}^{ii})\cdot\hat{\mathbf{e}}_p^*}{\hbar\omega_p} \quad (17)$$

greatly influences the THz radiation of the Rashba quantum ring.

The Schrödinger equation $i\hbar\frac{\partial}{\partial t}|\Psi(t)\rangle=\mathcal{H}_{\rm TLS}|\Psi(t)\rangle$ for the state vector of the electron $|\Psi(t)\rangle=c_i(t)|\Psi_i\rangle+c_f(t)|\Psi_f\rangle$ can be written as

$$\begin{aligned}i\hbar\dot{c}_i(t)&=c_i(t)\left(-\frac{\hbar\omega_{fi}}{2}+\mathcal{V}_{ii}e^{i\omega_p t}+\mathcal{V}_{ii}^\dagger e^{-i\omega_p t}\right)\\&\quad+c_f(t)(\mathcal{V}_{if}e^{i\omega_p t}+\mathcal{V}_{if}^\dagger e^{-i\omega_p t}),\\i\hbar\dot{c}_f(t)&=c_i(t)(\mathcal{V}_{fi}e^{i\omega_p t}+\mathcal{V}_{fi}^\dagger e^{-i\omega_p t})\\&\quad+c_f(t)\left(\frac{\hbar\omega_{fi}}{2}+\mathcal{V}_{ff}e^{i\omega_p t}+\mathcal{V}_{ff}^\dagger e^{-i\omega_p t}\right).\end{aligned} \quad (18)$$

We employ

$$\begin{aligned}\mathcal{X}_i(t)&=+i\frac{\omega_{fi}}{2}t-\frac{\mathcal{V}_{ii}e^{i\omega_p t}-\mathcal{V}_{ii}^\dagger e^{-i\omega_p t}}{\hbar\omega_p},\\\mathcal{X}_f(t)&=-i\frac{\omega_{fi}}{2}t-\frac{\mathcal{V}_{ff}e^{i\omega_p t}-\mathcal{V}_{ff}^\dagger e^{-i\omega_p t}}{\hbar\omega_p},\end{aligned} \quad (19)$$

to introduce the auxiliary functions $\tilde{c}_i(t)=e^{-\mathcal{X}_i(t)}c_i(t)$ and $\tilde{c}_f(t)=e^{-\mathcal{X}_f(t)}c_f(t)$. It follows that

$$\begin{aligned}i\hbar\dot{\tilde{c}}_i&=\tilde{c}_f(t)e^{\mathcal{X}_f(t)-\mathcal{X}_i(t)}(\mathcal{V}_{if}e^{i\omega_p t}+\mathcal{V}_{if}^\dagger e^{-i\omega_p t}),\\i\hbar\dot{\tilde{c}}_f&=\tilde{c}_i(t)e^{\mathcal{X}_i(t)-\mathcal{X}_f(t)}(\mathcal{V}_{fi}e^{i\omega_p t}+\mathcal{V}_{fi}^\dagger e^{-i\omega_p t}).\end{aligned} \quad (20)$$

The identity $e^{\frac{u}{2}(z-1/z)}=\sum_{n=-\infty}^{\infty}J_n(u)z^n$ allows us to write $e^{\mathcal{X}_f(t)-\mathcal{X}_i(t)}=e^{-i\omega_{fi}t}\sum_{n=-\infty}^{\infty}J_n(\kappa)e^{in\xi}e^{in\omega_p t}$. Hereafter, we assume that $\Delta=\omega_{fi}-m\omega_p$ is small (mth resonance) and

simplify the above set of coupled equations to

$$i\hbar\,\dot{\tilde{c}}_i(t) = [\mathcal{V}_{if}J_{m-1}(\kappa)e^{-i\xi} + \mathcal{V}_{if}^{\dagger}J_{m+1}(\kappa)e^{i\xi}]e^{im\xi}e^{-i\Delta t}\tilde{c}_f(t),$$
$$i\hbar\,\dot{\tilde{c}}_f(t) = [\mathcal{V}_{fi}^{\dagger}J_{m-1}(\kappa)e^{i\xi} + \mathcal{V}_{fi}J_{m+1}(\kappa)e^{-i\xi}]e^{-im\xi}e^{i\Delta t}\tilde{c}_i(t). \quad (21)$$

The coefficients of Eqs. (21) are still time dependent, thus we introduce the auxiliary functions $\mathcal{C}_i(t)=e^{+i\frac{\Delta}{2}t}\tilde{c}_i(t)$ and $\mathcal{C}_f(t)=e^{-i\frac{\Delta}{2}t}\tilde{c}_f(t)$. We find that

$$\dot{\mathcal{C}}_i = \frac{i\Delta}{2}\mathcal{C}_i - i\frac{\Omega_R^*}{2}\mathcal{C}_f,$$
$$\dot{\mathcal{C}}_f = -\frac{i\Delta}{2}\mathcal{C}_f - i\frac{\Omega_R}{2}\mathcal{C}_i, \quad (22)$$

where the Rabi frequency $\Omega_R = |\Omega_R|e^{i\xi_R}$ is

$$\Omega_R = \frac{2}{\hbar}\left[\mathcal{V}_{fi}^{\dagger}J_{m-1}(\kappa)e^{-i(m-1)\xi} + \mathcal{V}_{fi}J_{m+1}(\kappa)e^{-i(m+1)\xi}\right]. \quad (23)$$

Now it is straightforward to solve Eqs. (22) and write the probability amplitudes as

$$c_i(t) = \left(c_i(0)e^{-\chi_i(0)}\left[\cos\left(\frac{\Omega t}{2}\right) + \frac{i\Delta}{\Omega}\sin\left(\frac{\Omega t}{2}\right)\right] - ic_f(0)\frac{\Omega_R^*}{\Omega}e^{-\chi_f(0)}\sin\left(\frac{\Omega t}{2}\right)\right)e^{\chi_i(t)}e^{-i\frac{\Delta t}{2}},$$
$$c_f(t) = \left(-ic_i(0)\frac{\Omega_R}{\Omega}e^{-\chi_i(0)}\sin\left(\frac{\Omega t}{2}\right) + c_f(0)e^{-\chi_f(0)} \times\left[\cos\left(\frac{\Omega t}{2}\right) - \frac{i\Delta}{\Omega}\sin\left(\frac{\Omega t}{2}\right)\right]\right)e^{\chi_f(t)}e^{i\frac{\Delta t}{2}}, \quad (24)$$

where $\Omega = \sqrt{\Delta^2 + |\Omega_R|^2}$.

To describe the salient features of the electromagnetic wave scattered by the Rashba quantum ring, we treat it as an electric dipole with a dipole moment

$$\langle\Psi(t)|\boldsymbol{\mu}|\Psi(t)\rangle = \tfrac{1}{2}\langle\Psi_i|\boldsymbol{\mu}|\Psi_i\rangle + \tfrac{1}{2}(\langle\Psi_f|\boldsymbol{\mu}|\Psi_f\rangle - \langle\Psi_i|\boldsymbol{\mu}|\Psi_i\rangle)|c_f(t)|^2 + \langle\Psi_f|\boldsymbol{\mu}|\Psi_i\rangle c_f^*(t)c_i(t) + \text{c.c.} \quad (25)$$

Without loss of generality, hereafter we assume that $c_i(0) = 1$ and $c_f(0) = 0$. We find that

$$\langle\Psi(t)|\boldsymbol{\mu}|\Psi(t)\rangle = \frac{1}{2}\boldsymbol{\mu}^{ii} + \frac{|\Omega_R|^2}{2\Omega^2}(\boldsymbol{\mu}^{ff} - \boldsymbol{\mu}^{ii})\sin^2\left(\frac{\Omega t}{2}\right) + \frac{i\Omega_R^*}{\Omega}\boldsymbol{\mu}^{fi}\sin\left(\frac{\Omega t}{2}\right)\left[\cos\left(\frac{\Omega t}{2}\right) + \frac{i\Delta}{\Omega}\sin\left(\frac{\Omega t}{2}\right)\right] \times\sum_{n=-\infty}^{\infty}J_{m+n}(\kappa)e^{-i(m+n)\xi}e^{-in\omega_p t} + \text{c.c.} \quad (26)$$

A multitude of frequencies $n\omega_p$ and $n\omega_p \pm \sqrt{\Delta^2 + |\Omega_R|^2}$ $(n = 1, 2, ...)$ exist in the dipole emission spectrum. In particular, the Rashba quantum ring radiates at the frequency $\sqrt{\Delta^2 + |\Omega_R|^2}$ when $\boldsymbol{\mu}^{ff} - \boldsymbol{\mu}^{ii} \neq 0$. This is of prime importance, since the amplitude of the incident wave, the external static electric field, and the gate-voltage-dependent Rashba parameter can be adjusted to guarantee that $|\Omega_R|$ lies in the *terahertz* range.

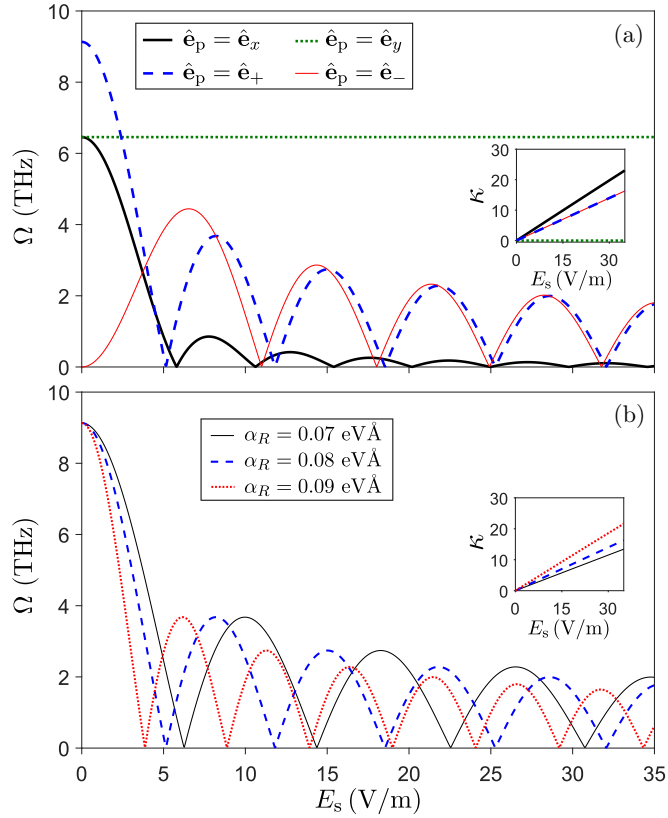

FIG. 5. Generalized Rabi frequency Ω versus static electric field E_s for (a) various incident polarizations when $\alpha_R = 0.08$ eVÅ, and (b) various Rashba parameters when $\hat{\mathbf{e}}_p = \hat{\mathbf{e}}_+$. The insets show the corresponding plots of asymmetry parameter κ versus E_s. Here $m^* = 0.067m_e$, $r_c = 85$ nm, $E_p = 10^5$ V/m, $\omega_p/(2\pi) = 8$ GHz and $m = 1$.

As a concrete example, we consider an InGaAs quantum ring of radius $r_c = 85$ nm. We assume that for given static electric field and Rashba parameter, $|\Psi_i\rangle$ and $|\Psi_f\rangle$ are $\psi_{0,-1}$-like ground state and $\psi_{+1,-1}$-like first excited state, respectively. We further assume that the amplitude and frequency of the incident wave are $E_p = 10^5$ V/m and $\omega_p/(2\pi) = 8$ GHz. We concentrate on the first resonance, that is $m = 1$. Figure 5(a) shows generalized Rabi frequency Ω as a function of E_s for various incident polarizations when $\alpha_R = 0.08$ eVÅ. It is apparent that for incident polarization vector $\hat{\mathbf{e}}_+$, the static electric field can be tuned to ensure that Ω lies in the range of 0.1−9.13 THz. For incident polarization vectors $\hat{\mathbf{e}}_x$ and $\hat{\mathbf{e}}_-$, the highest frequency radiations are at 6.46 and 4.44 THz, respectively. When the incident polarization vector is perpendicular to the static electric field, the generalized Rabi frequency is 6.46 THz. To emphasize the possibility of THz radiation in a range of gate voltages, Fig. 5(b) shows Ω as a function of E_s for three different Rashba parameters, when the polarization vector is $\hat{\mathbf{e}}_+$. It is apparent that static electric fields as low as 10 V/m can be utilized to warrant that Ω lies in the range of 0.1−9.13 THz. We conclude that a Rashba quantum ring may be utilized as an electrically tunable THz wave source.

VI. OPTICAL ACTIVITY OF A RASHBA QUANTUM RING

Now we consider a linearly polarized incident wave with polarization vector $\hat{\mathbf{e}}_\mathrm{p}=\cos\varphi\hat{\mathbf{e}}_x+\sin\varphi\hat{\mathbf{e}}_y$. Here we assume that the driving frequency is in the THz region. The electric field radiated by the quantum ring has a component $\mathrm{Re}(\mathbf{E}_\mathrm{r}e^{-i\omega_\mathrm{p}t})$ which oscillates at the driving frequency ω_p and propagates along the direction $\mathbf{k}_\mathrm{p}=k_\mathrm{p}\hat{\mathbf{e}}_z$. In general, this field is elliptically polarized. The vibration ellipse can be characterized by the azimuth φ_r and ellipticity $\tan\eta_r$. The polarization azimuth rotation $\varphi_r-\varphi$ and the ellipticity angle variation η_r describe the optical activity of the quantum ring at the driving frequency ω_p. Indeed,

$$\varphi_r=\frac{1}{2}\arctan\left(\frac{S_2}{S_1}\right),$$
$$\eta_r=\frac{1}{2}\arcsin\left(-\frac{S_3}{S_0}\right), \tag{27}$$

where $S_0=|E_{rx}|^2+|E_{ry}|^2$, $S_1=|E_{rx}|^2-|E_{ry}|^2$, $S_2=2\mathrm{Re}(E_{rx}E_{ry}^*)$, and $S_3=2\mathrm{Im}(E_{rx}E_{ry}^*)$ are the Stokes parameters [51]. We confine our attention to the case $m=1$, i.e., the first resonance. According to Eq. (26), the effective dipole moment of the system has a component $\mathrm{Re}(\mathbf{d}_\mathrm{cl}e^{-i\omega_\mathrm{p}t})$, where

$$\mathbf{d}_\mathrm{cl}=-\frac{|\Omega_R|\Delta}{\Omega^2}(J_0(\kappa)e^{i\xi_R}\boldsymbol{\mu}^{fi^*}+J_2(\kappa)e^{-2i\xi-i\xi_R}\boldsymbol{\mu}^{fi}). \tag{28}$$

We measure the electric field radiated by the quantum ring at a point $h\hat{\mathbf{e}}_z$ where $h\gg 1/k_\mathrm{p}\gg r_\mathrm{c}$. Indeed $\mathbf{E}_\mathrm{r}\propto\mathbf{d}_\mathrm{cl}$ in the far (radiation) zone, thus φ_r and η_r ultimately depend on the external static electric field E_s and the Rashba parameter α_R.

As before, we assume that $|\Psi_i\rangle$ and $|\Psi_f\rangle$ are $\psi_{0,-1}$-like ground state and $\psi_{+1,-1}$-like first excited state, respectively. We further assume that $m^*=0.067m_e$, $r_\mathrm{c}=40$ nm, $E_\mathrm{p}=10^5$ V/m, $\Delta=-0.1\omega_{fi}$, and $m=1$. Figures 6(a) and 6(b) demonstrate $\varphi_r-\varphi$ and η_r as a function of φ for $E_\mathrm{s}=2000$ V/m and various Rashba parameters. Here $\omega_\mathrm{p}/(2\pi)$ is about 0.081−0.087 THz. Quite remarkably, $\varphi_r-\varphi=90^\circ$ when $0<\varphi<\varphi_{c1}$, and $\varphi_r-\varphi=-90^\circ$ when $\varphi_{c2}<\varphi<180^\circ$. Indeed both $\varphi_{c1}\approx 45^\circ$ and $\varphi_{c2}\approx 135^\circ$ weakly depend on the Rashba parameter. For $\varphi_{c1}<\varphi<\varphi_{c2}$, we find that the polarization azimuth rotation $\varphi_r-\varphi$ is small. The radiated field is almost linearly polarized when $\varphi=0^\circ$, almost right-circularly polarized when $\varphi=90^\circ$, and almost left-circularly polarized when $\varphi=\varphi_{c1}$ or φ_{c2}. Figures 6(c) and 6(d) show $\varphi_r-\varphi$ and η_r as a function of E_s when $\varphi=0^\circ$ ($\varphi=90^\circ$) and the polarization vector is parallel (perpendicular) to the static electric field. Here $\alpha_\mathrm{R}=0.08$ eVÅ and $\Delta=-0.1\omega_{fi}$, thus $\omega_\mathrm{p}/(2\pi)$ is about 0.081−0.114 THz as the static electric field varies. For $\varphi=0^\circ$ indeed polarization rotation $\varphi_r-\varphi$ is 0° (90°) for static electric fields smaller (larger) than a threshold 1291 V/m. The radiated field is right-circularly polarized for $E_\mathrm{s}=0$, linearly polarized for $E_\mathrm{s}=980$ and 2339 V/m, and left-circularly polarized for the threshold field 1291 V/m. Quite interestingly, the polarization rotation $\varphi_r-\varphi$ is zero when $\varphi=90^\circ$. Here the static electric field merely influences the ellipticity of the radiated field. We conclude that a Rashba quantum ring may serve as an electrically tunable THz polarization rotator.

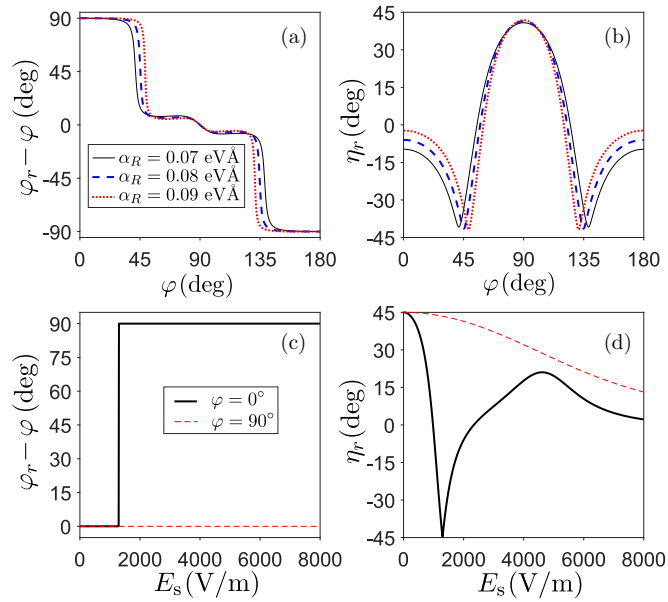

FIG. 6. (a) $\varphi_r-\varphi$ and (b) η_r as a function of φ when $E_\mathrm{s}=2000$ V/m. (c) $\varphi_r-\varphi$ and (d) η_r as a function of E_s when $\alpha_\mathrm{R}=0.08$ eVÅ. In all plots, $m^*=0.067m_e$, $r_\mathrm{c}=40$ nm, $E_\mathrm{p}=10^5$ V/m, $\Delta=-0.1\omega_{fi}$, and $m=1$.

VII. CONCLUSION

A few remarks are in order.

(i) The absorption spectrum depends on the initial state of the system. For example, the absorption spectrum for the $\psi_{-1,-1}$-like initial state Ψ_II and incident polarization vector $\hat{\mathbf{e}}_+$ ($\hat{\mathbf{e}}_-$) is the same as the absorption spectrum for the $\psi_{0,-1}$-like initial state Ψ_I and incident polarization vector $\hat{\mathbf{e}}_-$ ($\hat{\mathbf{e}}_+$).

(ii) Eldridge *et al.* have performed *all-optical* spin-dynamic measurement of the Rashba interaction in GaAs/AlGaAs *quantum wells* under an applied electric field [52]. Figure 4 shows that the linear and circular dichroism spectra of a Rashba quantum ring strongly depend on the Rashba interaction and the external electric field. This may provide a route toward all-optical measurement of the Rashba parameter.

(iii) The electric dipole moment of a Rashba quantum ring is proportional to its radius $r_\mathrm{c}\sim 40-80$ nm. This allows the system to radiate as a *giant* artificial atom.

(iv) Here it is shown that the superposition of quantum states of different angular momentum quantum numbers ultimately allows the system to exhibit linear dichroism and to radiate at the Rabi frequency. It is noteworthy that mixing quantum states of different parities was recently proposed for the induction of optical activity in achiral nanostructures [53].

(v) The asymmetry parameter κ of a quantum dot or a quantum well is about 0.01 [13,15]. Remarkably, κ of a Rashba quantum ring may be as large as 20 [see insets in Fig. 5]. Thus, to develop THz emitters based on asymmetric artificial atoms, quantum dots and quantum wells may be inferior to Rashba quantum rings.

(vi) The asymmetry parameter depends on the amplitude, frequency, and polarization of the driving field, the static electric field, and gate-voltage-dependent Rashba parameter [see Eq. (17)]. If $\mathcal{V}_{fi}^\dagger J_0(\kappa)+\mathcal{V}_{fi}J_2(\kappa)e^{-2i\xi}=0$, then the Rabi

frequency associated with the first resonance and the emission at frequency $\sqrt{\Delta^2+|\Omega_R|^2}$ are suppressed [see Eqs. (23) and (26), and Fig. 5].

(vii) A singlet at the frequency $\sqrt{\Delta^2+|\Omega_R|^2}$ and an infinite sequence of triplets with the frequencies $n\omega_{\rm p}$ and $n\omega_{\rm p}\pm\sqrt{\Delta^2+|\Omega_R|^2}$ $(n=1,2,...)$ exist in the radiation spectrum [see Eq. (26)]. This suggests that the Rashba quantum ring can be utilized for the high harmonic generation. Indeed, both even and odd harmonics can be generated. Nevertheless, the amplitude of the nth harmonic decreases as n increases.

(viii) We have focused on the unitary evolution of the system described by the Hamiltonian $\mathcal{H}_{\rm TLS}$ [see Eq. (18)]. In other words, we have considered the strong coupling regime $\Omega_R\tau\gg1$, where the relaxation constant τ describes the system-environment interaction. Even for a linewidth as large as $\tau^{-1}=0.1\omega_{fi}\approx5$ GHz, we find that $\Omega_R\tau\approx20-2000$, thus the strong coupling regime can be reached.

In conclusion, we have studied a Rashba quantum ring subjected to a static electric field. Interacting with a strong electromagnetic field, the Rashba quantum ring radiates at the Rabi frequency. The Rabi frequency is proportional to the driving field amplitude, thus THz emission is achievable. Moreover, the external static electric field, the gate-voltage-dependent Rashba parameter, and the frequency and polarization of the driving field can be used to control the THz emission. In the THz region of the electromagnetic spectrum, the absorption, static electric field-induced linear dichroism, and Rashba interaction-induced circular dichroism and optical activity of the system are considerable and markedly influenced by the external field and gate voltage. Thus the Rashba quantum ring is promising for realizing electrically tunable terahertz emitter, absorption modulator, dichroic element, and polarization rotator.

APPENDIX: DOUBLY DEGENERATE GROUND STATES OF A RASHBA RING

Equation (10) grants access to the ground-state energy and doubly degenerate wave functions of a Rashba quantum ring. To name the doubly degenerate ground states, we adopt the following convention: $\Psi_{\rm I}$ ($\Psi_{\rm II}$) is a $\psi_{0,-1}$-like ($\psi_{-1,-1}$-like) wave function. Here we assume that $m^*=0.067m_e$, $r_{\rm c}=40$ nm, and $\alpha_{\rm R}=0.08$ eVÅ.

When $E_{\rm s}=0$,

$$\mathcal{E}=-0.026\ \text{meV},\quad \Psi_{\rm I}=\psi_{0,-1},\quad \Psi_{\rm II}=\psi_{-1,-1}. \tag{A1}$$

When $E_{\rm s}=2000$ V/m,

$$\begin{aligned}\mathcal{E}=&-0.035\ \text{meV},\\ \Psi_{\rm I}=&-0.002\psi_{-2,1}+0.095\psi_{-1,1}+0.987\psi_{0,-1}\\ &-0.127\psi_{1,-1}+0.004\psi_{2,-1},\\ \Psi_{\rm II}=&+0.004\psi_{-3,-1}-0.127\psi_{-2,-1}+0.987\psi_{-1,-1}\\ &-0.095\psi_{0,1}+0.002\psi_{1,1}.\end{aligned} \tag{A2}$$

When $E_{\rm s}=4000$ V/m,

$$\begin{aligned}\mathcal{E}=&-0.060\ \text{meV},\\ \Psi_{\rm I}=&-0.009\psi_{-2,1}+0.175\psi_{-1,1}+0.957\psi_{0,-1}\\ &-0.231\psi_{1,-1}+0.014\psi_{2,-1},\\ \Psi_{\rm II}=&+0.014\psi_{-3,-1}-0.231\psi_{-2,-1}+0.957\psi_{-1,-1}\\ &-0.175\psi_{0,1}+0.009\psi_{1,1}.\end{aligned} \tag{A3}$$

When $E_{\rm s}=6000$ V/m,

$$\begin{aligned}\mathcal{E}=&-0.097\ \text{meV},\\ \Psi_{\rm I}=&-0.018\psi_{-2,1}+0.236\psi_{-1,1}+0.922\psi_{0,-1}\\ &-0.305\psi_{1,-1}+0.026\psi_{2,-1}-0.001\psi_{3,-1},\\ \Psi_{\rm II}=&-0.001\psi_{-4,-1}+0.026\psi_{-3,-1}-0.305\psi_{-2,-1}\\ &+0.922\psi_{-1,-1}-0.236\psi_{0,1}+0.018\psi_{1,1}.\end{aligned} \tag{A4}$$

When $E_{\rm s}=8000$ V/m,

$$\begin{aligned}\mathcal{E}=&-0.141\ \text{meV},\\ \Psi_{\rm I}=&+0.001\psi_{-3,1}-0.028\psi_{-2,1}+0.281\psi_{-1,1}\\ &+0.890\psi_{0,-1}-0.356\psi_{1,-1}+0.040\psi_{2,-1}\\ &-0.002\psi_{3,-1},\\ \Psi_{\rm II}=&-0.002\psi_{-4,-1}+0.040\psi_{-3,-1}-0.356\psi_{-2,-1}\\ &+0.890\psi_{-1,-1}-0.281\psi_{0,1}+0.028\psi_{1,1}\\ &-0.001\psi_{2,1}.\end{aligned} \tag{A5}$$

[1] Y.-S. Lee, *Principles of Terahertz Science and Technology* (Springer, New York, 2009).

[2] X.-C. Zhang and J. Xu, *Introduction to THz Wave Photonics* (Springer, New York, 2010).

[3] R. A. Kaindl, M. A. Carnahan, J. Orenstein, D. S. Chemla, H. M. Christen, H.-Y. Zhai, M. Paranthaman, and D. H. Lowndes, Far-Infrared Optical Conductivity Gap in Superconducting MgB_2 Films, Phys. Rev. Lett. **88**, 027003 (2002).

[4] R. A. Kaindl, M. A. Carnahan, D. Hägele, R. Lövenich, and D. S. Chemla, Ultrafast terahertz probes of transient conducting and insulating phases in an electron-hole gas, Nature **423**, 734 (2003).

[5] T. Kampfrath, A. Sell, G. Klatt, A. Pashkin, S. Mahrlein, T. Dekorsy, M. Wolf, M. Fiebig, A. Leitenstorfer, and R. Huber, Coherent terahertz control of antiferromagnetic spin waves, Nat. Photon. **5**, 31 (2011).

[6] H. Eisele, A. Rydberg, and G. I. Haddad, Recent advances in the performance of InP Gunn devices and GaAs TUNNETT diodes for the 100-300-GHz frequency range and above, IEEE Trans. Microwave Theory Tech. **48**, 626 (2000).

[7] O. V. Kibis, M. Rosenau da Costa, and M. E. Portnoi, Generation of terahertz radiation by hot electrons in carbon nanotubes, Nano Lett **7**, 3414 (2007).

[8] V. Ryzhii, A. A. Dubinov, V. Y. Aleshkin, M. Ryzhii, and T. Otsuji, Injection terahertz laser using the resonant inter-layer

radiative transitions in double-graphene-layer structure, Appl. Phys. Lett. **103**, 163507 (2013).

[9] T. C. H. Liew, M. M. Glazov, K. V. Kavokin, I. A. Shelykh, M. A. Kaliteevski, and A. V. Kavokin, Proposal for a Bosonic Cascade Laser, Phys. Rev. Lett. **110**, 047402 (2013).

[10] S. De Liberato, C. Ciuti, and C. C. Phillips, Terahertz lasing from intersubband polariton-polariton scattering in asymmetric quantum wells, Phys. Rev. B **87**, 241304(R) (2013).

[11] O. Kyriienko, A. V. Kavokin, and I. A. Shelykh, Superradiant Terahertz Emission by Dipolaritons, Phys. Rev. Lett. **111**, 176401 (2013).

[12] J. Wu, S. Chen, A. Seeds, and H. Liu, Quantum dot optoelectronic devices: Lasers, photodetectors and solar cells, J. Phys. D: Appl. Phys. **48**, 363001 (2015).

[13] O. V. Kibis, G. Ya. Slepyan, S. A. Maksimenko, and A. Hoffmann, Matter Coupling to Strong Electromagnetic Fields in Two-Level Quantum Systems with Broken Inversion Symmetry, Phys. Rev. Lett. **102**, 023601 (2009).

[14] I. Yu. Chestnov, V. A. Shahnazaryan, A. P. Alodjants, and I. A. Shelykh, Terahertz lasing in ensemble of asymmetric quantum dots, ACS Photonics **4**, 2726 (2017).

[15] N. Shammah, C. C. Phillips, and S. De Liberato, Terahertz emission from ac Stark-split asymmetric intersubband transitions, Phys. Rev. B **89**, 235309 (2014).

[16] M. F. Miri, F. Zamani, and H. Alipoor, Two tunneling-coupled two-level systems with broken inversion symmetry: Tuning the terahertz emission, J. Opt. Soc. Am. B **33**, 1873 (2016).

[17] F. Zamani and M. F. Miri, Terahertz emission from an array of tunneling-coupled asymmetric two-level systems, Opt. Commun. **423**, 207 (2018).

[18] V. M. Fomin, *Physics of Quantum Rings* (Springer, Berlin, 2014).

[19] T. Ihn, *Semiconductor Nanostructures: Quantum States and Electronic Transport* (Oxford University Press, Oxford, 2010).

[20] Y. Aharonov and D. Bohm, Significance of electromagnetic potentials in the quantum theory, Phys. Rev. **115**, 485 (1959).

[21] Y. Aharonov and A. Casher, Topological Quantum Effects for Neutral Particles, Phys. Rev. Lett. **53**, 319 (1984).

[22] R. A. Webb, S. Washburn, C. P. Umbach, and R. B. Laibowitz, Observation of h/e Aharonov-Bohm Oscillations in Normal-Metal Rings, Phys. Rev. Lett. **54**, 2696 (1985).

[23] G. Timp, A. M. Chang, J. E. Cunningham, T. Y. Chang, P. Mankiewich, R. Behringer, and R. E. Howard, Observation of the Aharonov-Bohm effect for $\omega_c\tau > 1$, Phys. Rev. Lett. **58**, 2814 (1987).

[24] S. Pedersen, A. E. Hansen, A. Kristensen, C. B. Sørensen, and P. E. Lindelof, Observation of quantum asymmetry in an Aharonov-Bohm ring, Phys. Rev. B **61**, 5457 (2000).

[25] M. König, A. Tschetschetkin, E. M. Hankiewicz, Jairo Sinova, V. Hock, V. Daumer, M. Schäfer, C. R. Becker, H. Buhmann, and L. W. Molenkamp, Direct Observation of the Aharonov-Casher Phase, Phys. Rev. Lett. **96**, 076804 (2006).

[26] F. Nagasawa, D. Frustaglia, H. Saarikoski, K. Richter, and J. Nitta, Control of the spin geometric phase in semiconductor quantum rings, Nat. Commun. **4**, 2526 (2013).

[27] Y. A. Bychkov and E. I. Rashba, Properties of a 2D electron gas with lifted spectral degeneracy, Pis'ma Zh. Eksp. Teor. Fiz. **39**, 66 (1984).

[28] A. Manchon, H. C. Koo, J. Nitta, S. M. Frolov, and R. A. Duine, New perspectives for Rashba spin-orbit coupling, Nat. Mater. **14**, 871 (2015).

[29] D. Bercioux and P. Lucignano, Quantum transport in Rashba spin-orbit materials: A review, Rep. Prog. Phys. **78**, 106001 (2015).

[30] S. M. Huang, A. O. Badrutdinov, L. Serra, T. Kodera, T. Nakaoka, N. Kumagai, Y. Arakawa, D. A. Tayurskii, K. Kono, and K. Ono, Enhancement of Rashba coupling in vertical $In_{0.05}Ga_{0.95}As/GaAs$ quantum dots, Phys. Rev. B **84**, 085325 (2011).

[31] J. Nitta, T. Akazaki, H. Takayanagi, and T. Enoki, Gate Control of Spin-Orbit Interaction in an Inverted $In_{0.53}Ga_{0.47}As/In_{0.52}Al_{0.48}As$ Heterostructure, Phys. Rev. Lett. **78**, 1335 (1997).

[32] M. Schultz, F. Heinrichs, U. Merkt, T. Colin, T. Skauli, and S. Løvold, Rashba spin splitting in a gated HgTe quantum well, Semicond. Sci. Technol. **11**, 1168 (1996).

[33] H. C. Koo, J. H. Kwon, J. H. Eom, J. Y. Chang, S. H. Han, and M. Johnson, Control of spin precession in a spin-injected field effect transistor, Science **325**, 1515 (2009).

[34] Y. H. Park, H. Kim, J. Chang, S. H. Han, J. Eom, H. Choi, and H. C. Koo, Separation of Rashba and Dresselhaus spin-orbit interactions using crystal direction dependent transport measurements, Appl. Phys. Lett. **103**, 252407 (2013).

[35] G. F. Quinteiro, A. O. Lucero, and P. I. Tamborenea, Electronic transitions in quantum dots and rings induced by inhomogeneous off-centered light beams, J. Phys. Condens. Matter **22**, 505802 (2010).

[36] A. M. Alexeev and M. E. Portnoi, Electric dipole moment oscillations in Aharonov-Bohm quantum rings, Phys. Rev. B **85**, 245419 (2012).

[37] A. M. Alexeev, I. A. Shelykh, and M. E. Portnoi, Aharonov-Bohm quantum rings in high-Q microcavities, Phys. Rev. B **88**, 085429 (2013).

[38] F. K. Joibari, Y. M. Blanter, G. E. W. Bauer, Light-induced spin polarizations in quantum rings, Phys. Rev. B **90**, 155301 (2014).

[39] H. Sigurdsson, O. V. Kibis, and I. A. Shelykh, Optically induced Aharonov-Bohm effect in mesoscopic rings, Phys. Rev. B **90**, 235413 (2014).

[40] M. Hasan, I. V. Iorsh, O. V. Kibis, and I. A. Shelykh, Optically controlled periodical chain of quantum rings, Phys. Rev. B **93**, 125401 (2016).

[41] V. K. Kozin, I. V. Iorsh, O. V. Kibis, and I. A. Shelykh, Periodic array of quantum rings strongly coupled to circularly polarized light as a topological insulator, Phys. Rev. B **97**, 035416 (2018).

[42] V. K. Kozin, I. V. Iorsh, O. V. Kibis, and I. A. Shelykh, Quantum ring with the Rashba spin-orbit interaction in the regime of strong light-matter coupling, Phys. Rev. B **97**, 155434 (2018).

[43] L. D. Barron and C. G. Gray, The multipole interaction Hamiltonian for time dependent fields, J. Phys. A **6**, 59 (1973).

[44] L. Novotny and B. Hecht, *Principles of Nano-Optics* (Cambridge University Press, Cambridge, 2006).

[45] F. E. Meijer, A. F. Morpurgo, and T. M. Klapwijk, One-dimensional ring in the presence of Rashba spin-orbit interaction: Derivation of the correct Hamiltonian, Phys. Rev. B **66**, 033107 (2002).

[46] A. Lorke, R. J. Luyken, A. O. Govorov, J. P. Kotthaus, J. M. Garcia, and P. M. Petroff, Spectroscopy of Nanoscopic Semiconductor Rings, Phys. Rev. Lett. **84**, 2223 (2000).

[47] W. Lei, C. Notthoff, A. Lorke, D. Reuter, and A. D. Wieck, Electronic structure of self-assembled InGaAs/GaAs quantum rings studied by capacitance-voltage spectroscopy, Appl. Phys. Lett. **96**, 033111 (2010).

[48] D. Granados, J. M. García, T. Ben, and S. I. Molina, Vertical order in stacked layers of self-assembled In(Ga)As quantum rings on GaAs (001), Appl. Phys. Lett. **86**, 071918 (2005).

[49] P. Offermans, P. M. Koenraad, J. H. Wolter, D. Granados, J. M. García, V. M. Fomin, V. N. Gladilin, and J. T. Devreese, Atomic-scale structure of self-assembled In(Ga)As quantum rings in GaAs, Appl. Phys. Lett. **87**, 131902 (2005).

[50] Z. Gong, Z. C. Niu, S. S. Huang, Z. D. Fang, B. Q. Sun, and J. B. Xia, Formation of GaAs/AlGaAs and InGaAs/GaAs nanorings by droplet molecular-beam epitaxy, Appl. Phys. Lett. **87**, 093116 (2005).

[51] F. Borghese, P. Denti, and R. Saija, *Scattering from Model Nonspherical Particles* (Springer, Berlin, 2007).

[52] P. S. Eldridge, W. J. H. Leyland, P. G. Lagoudakis, O. Z. Karimov, M. Henini, D. Taylor, R. T. Phillips, and R. T. Harley, All-optical measurement of Rashba coefficient in quantum wells, Phys. Rev. B **77**, 125344 (2008).

[53] A. S. Baimuratov, N. V. Tepliakov, Y. K. Gun'ko, A. V. Baranov, A. V. Fedorov, and I. D. Rukhlenko, Mixing of quantum states: A new route to creating optical activity, Sci. Rep. **6**, 17 (2016).